THE ASTROPHYSICAL JOURNAL, 295: 537–546, 1985 August 15

APPARENT MAGNITUDES OF LUMINOUS PLANETARY NEBULA NUCLEI. I. METHOD AND APPLICATION

RICHARD A. SHAW AND JAMES B. KALER
Astronomy Department, University of Illinois
Received 1984 December 26; accepted 1985 February 25

ABSTRACT

We present new *B*- and/or *V*-magnitudes for the nuclei of 51 planetary nebulae, as well as limits for 10 others, from absolute photometry with the University of Illinois 1 m telescope, and a superior method of extracting stellar continuum fluxes from a bright nebular background. The errors and the limitations of the method are carefully examined.

We compare the results with the widely circulated list of preliminary central-star magnitudes determined by Shao and Liller, which are shown to suffer frequently from severe contamination from the nebular continuum, and we provide a calibration for older photographic magnitudes. Finally, we examine the nebular contribution to the continuum in the context of the evolution of central stars on the log *L*–log *T* plane and discuss the implications for future observations of hot and/or young planetary nuclei.

Subject headings: nebulae: planetary — photometry — stars: early-type

I. INTRODUCTION AND METHOD

The correct determination of continuum fluxes from hot stars embedded within bright planetary nebulae has proved to be somewhat elusive. The contribution to the total continuum flux from the surrounding nebula has been consistently underestimated or even ignored by many investigators. The resulting incorrect stellar fluxes confound efforts to chart the evolution of planetary nuclei through the log *L*–log *T* plane during the most rapid—and in some respects crucial—phase of that evolution.

Webster (1969) appears to have been the first to attempt to extract the stellar magnitude from the total continuum. She estimated the nebular contribution from her measured Hβ flux and relatively crude theory. The more detailed technique that we use here was developed and described by Kaler (1976*a*, 1978) and is summarized below. Martin (1981) also used a similar procedure.

In our method, the Hβ and the $\lambda\lambda$4428 and 5500 (Strömgren *y*) continuum fluxes are observed through a common aperture. The nebular continuum flux at these wavelengths is then calculated from the observed Hβ flux, Brocklehurst's (1971) effective recombination coefficients, and the tables of Brown and Mathews (1970), for which we need (1) the electron temperature T_e; (2) the ionic helium abundances, He^+/H^+ and He^{2+}/H^+; and (3) the extinction constant, *c* (used with the Whitford 1958 reddening function), which allows us to find the reddened theoretical continuum at our observed wavelengths. The result is then subtracted from the total continuum, leaving stellar fluxes that are converted to *B*- and *V*-magnitudes. To good precision, the *y*-magnitude can be identified as *V*, and only a minor correction ($\lesssim$0.15 mag) for the effective filter wavelength is needed for *B*, which depends upon the color excess of the nucleus.

In this work, we primarily examine over 10 years' worth of data that were accumulated from wide-aperture surveys of planetaries, the original purpose of which was the measurement of absolute line fluxes. However, stellar continuum data are a natural by-product, and even though the observing technique was not optimized for the determination of magnitudes, there is a wealth of data from which they can still be extracted. In the following sections we revise the magnitudes published earlier and present a number of new measurements. We discuss the observations and their reduction in § II and present comparisons with other data in § III. Zanstra temperatures and the significance of the data to the study of stellar evolution are examined in § IV.

II. OBSERVATIONS AND REDUCTIONS

The observations were taken with the University of Illinois 1 m telescope at Prairie (later Mount Laguna) Observatory between 1971 and 1982. The observing technique has been described by Kaler (1976*a*). We use the data accumulated for that paper and for the studies also presented by Kaler (1978, 1980, 1983*a*, *b*), as well as some taken expressly for this program. All of the Prairie data have been rereduced using improved calibrations of the interference filters (see Shaw and Kaler 1982), as well as corrections for the effect of ambient temperature on the filter transmission functions. We also examined photographs of each program object in order to exclude those with field star contamination and, for the newly acquired data, to choose an appropriate aperture.

In columns (1) and (2) of Table 1 we list the objects that were observed and the corresponding Perek and Kohoutek (1967) designations. We give the adopted parameters in the next five columns: column (3) contains *c*, the extinction constant, while columns (4)–(7) give, in order, t ($=10^{-4}$ times the nebular electron temperature T_e), the log of the mean nebular density, and the ratios of singly and doubly ionized helium to ionized hydrogen, each with its associated uncertainty. These data are taken from the following sources: Kaler (1978, 1979, 1980, 1983*a*); the calculations made for the review by Kaler (1983*c*); calculations using the methodology and atomic parameters of the preceding references and line intensities from the references in Kaler (1976*b*, 1985), Torres-Peimbert and Peimbert (1977), Barker (1978), Aller and Czyzak (1979), and as yet unpublished Kitt Peak intensified Reticon scanner (IRS) and intensified image dissector scanner (IIDS) observations. If no measured data are available, parameters are simply assumed on the basis

TABLE 1

ADOPTED NEBULAR PHYSICAL PARAMETERS

Object (1)	PK[a] (2)	c (3)	t (4)	log N_e (5)	He^+/H^+ (6)	He^{2+}/H^+ (7)
NGC 650	130−10°1	0.15 ± 0.0	1.18 ± 0.10	3.75	0.079 ± 0.000	0.025 ± 0.001
NGC 1360	220−53°1	0.0 ± 0.0	1.80 ± 0.20	1.7	0.02 ± 0.01	0.090 ± 0.002
NGC 1501	144+06°1	1.0 ± 0.2	1.08 ± 0.20	...	0.112 ± 0.010	0.270 ± 0.005
NGC 1514	165−15°1	0.92 ± 0.10	1.42 ± 0.20	2.4	0.084 ± 0.010	0.016 ± 0.008
NGC 2392	197+17°1	0.16 ± 0.00	1.42 ± 0.10	3.43	0.049 ± 0.004	0.043 ± 0.002
NGC 2440	234+02°1	0.17 ± 0.00	1.30 ± 0.05	3.11	0.84 ± 0.000	0.069 ± 0.004
NGC 6058	64+48°1	0.05 ± 0.05	1.34 ± 0.05	3.74	0.04 ± 0.00	0.049 ± 0.005
NGC 6210	43+37°1	0.09 ± 0.07	0.96 ± 0.10	3.71	0.097 ± 0.000	0.002 ± 0.000
NGC 6309	9+14°1	0.07 ± 0.10	1.35 ± 0.05	3.62	0.040 ± 0.032	0.061 ± 0.007
NGC 6537	10+00°1	2.02 ± 0.14	1.60 ± 0.20	3.60	0.20 ± 0.12	0.070 ± 0.005
NGC 6543	96+29°1	0.12 ± 0.02	0.81 ± 0.10	3.86	0.105 ± 0.000	0.00 ± 0.00
NGC 6629	9−05°1	1.04 ± 0.17	0.85 ± 0.05	3.26	0.13 ± 0.03	0.00 ± 0.00
NGC 6644	8−07°2	0.41 ± 0.03	1.22 ± 0.10	3.86	0.091 ± 0.000	0.025 ± 0.001
NGC 6751	29−05°1	0.86 ± 0.30	1.00 ± 0.10	3.0	0.107 ± 0.000	0.00 ± 0.00
NGC 6807	42−06°1	0.33 ± 0.15	1.17 ± 0.10	3.6	0.103 ± 0.015	0.0 ± 0.0
NGC 6818	25−17°1	0.32 ± 0.05	1.27 ± 0.10	3.58	0.050 ± 0.006	0.043 ± 0.003
NGC 6826	83+12°1	0.04 ± 0.04	0.97 ± 0.05	3.21	0.095 ± 0.000	0.00 ± 0.00
NGC 6881	74+02°1	1.77 ± 0.18	1.41 ± 0.10	4.00	0.119 ± 0.020	0.032 ± 0.000
NGC 6884	82+07°1	0.81 ± 0.05	0.92 ± 0.20	3.90	0.095 ± 0.000	0.017 ± 0.005
NGC 6891	54−12°1	0.30 ± 0.10	1.00 ± 0.10	3.40	0.112 ± 0.00	0.00 ± 0.00
NGC 7008	93+05°2	0.84 ± 0.14	1.10 ± 0.20	3.60	0.033 ± 0.030	0.097 ± 0.000
NGC 7026	89+00°1	0.65 ± 0.15	0.88 ± 0.05	3.53	0.093 ± 0.000	0.010 ± 0.004
NGC 7354	107+02°1	1.76 ± 0.13	1.20 ± 0.20	3.8	0.080 ± 0.022	0.037 ± 0.001
NGC 7662	106−17°1	0.15 ± 0.03	1.30 ± 0.10	3.69	0.071 ± 0.000	0.042 ± 0.002
IC 289	138+02°1	1.15 ± 0.16	1.70 ± 0.20	2.7	0.015 ± 0.015	0.095 ± 0.010
IC 418	215−24°1	0.32 ± 0.03	0.94 ± 0.05	4.0	0.076 ± 0.000	0.00 ± 0.00
IC 1454	117+18°1	0.20 ± 0.10	1.00 ± 0.10	1.92	0.070 ± 0.01	0.02 ± 0.00
IC 2003	161−14°1	0.41 ± 0.06	1.19 ± 0.10	3.57	0.064 ± 0.000	0.042 ± 0.005
IC 2149	166+10°1	0.28 ± 0.13	1.10 ± 0.10	3.26	0.076 ± 0.000	0.00 ± 0.00
IC 2165	221−12°1	0.48 ± 0.02	1.34 ± 0.10	3.64	0.071 ± 0.010	0.041 ± 0.003
IC 3568	123+34°1	0.18 ± 0.01	1.08 ± 0.05	3.74	0.091 ± 0.000	0.001 ± 0.000
IC 4593	25+40°1	0.12 ± 0.08	0.88 ± 0.05	3.77	0.087 ± 0.000	0.00 ± 0.00
IC 4732	10−06°1	0.47 ± 0.20	1.44 ± 0.10	3.43	0.104 ± 0.019	0.00 ± 0.00
IC 4776	2−13°1	0.50 ± 0.50	1.00 ± 0.50	3.65	0.10 ± 0.01	0.00 ± 0.00
IC 5117	89−05°1	1.38 ± 0.10	1.12 ± 0.05	4.0	0.098 ± 0.010	0.008 ± 0.000
A2	122−04°1	0.37 ± 0.17	1.20 ± 0.20	2.00	0.046 ± 0.030	0.054 ± 0.018
A15	233−16°1	0.04 ± 0.15	1.60 ± 0.20	2.0	0.00 ± 0.00	0.114 ± 0.015
A33	238+34°1	0.00 ± 0.28	1.00 ± 0.10	2.0	0.09 ± 0.02	0.01 ± 0.00
A43	36+17°1	0.38 ± 0.22	1.40 ± 0.20	2.0	0.029 ± 0.020	0.081 ± 0.005
A46	55+16°1	0.00 ± 0.23	1.00 ± 0.10	2.0	0.10 ± 0.02	0.00 ± 0.00
A77	97+03°1	2.34 ± 0.13	1.00 ± 0.10	2.0	0.10 ± 0.02	0.00 ± 0.01
A79	102−02°1	1.40 ± 1.20	1.00 ± 0.10	2.0	0.10 ± 0.02	0.00 ± 0.01
Ha 3-29	174−14°1	1.17 ± 0.16	1.60 ± 0.20	3.0	0.00 ± 0.00	0.113 ± 0.010
HB 12	111−02°1	0.98 ± 0.20	1.40 ± 0.40	5.6	0.10 ± 0.02	0.00 ± 0.00
Hu 1-2	86−08°1	0.59 ± 0.02	1.76 ± 0.18	3.89	0.066 ± 0.010	0.098 ± 0.005
Hu 2-1	57+08°1	0.49 ± 0.02	0.91 ± 0.05	3.98	0.082 ± 0.010	0.00 ± 0.00
J320	190−17°1	0.22 ± 0.05	1.25 ± 0.10	3.62	0.102 ± 0.000	0.001 ± 0.000
J900	194+02°1	0.63 ± 0.13	1.21 ± 0.10	3.76	0.07 ± 0.01	0.036 ± 0.004
K3-63	98+02°1	1.04 ± 0.27	1.40 ± 0.20	3.0	0.023 ± 0.020	0.077 ± 0.010
M1-2	133−08°1	0.98 ± 0.25	1.50 ± 0.05	6.0	0.10 ± 0.02	0.00 ± 0.01
M1-4	147−02°1	1.36 ± 0.22	1.00 ± 0.10	4.0	0.085 ± 0.020	0.015 ± 0.010
M1-11	232−04°1	1.57 ± 0.13	1.00 ± 0.10	4.8	0.10 ± 0.02	0.00 ± 0.00
M2-51	103+00°1	1.39 ± 0.19	1.00 ± 0.10	2.6	0.088 ± 0.020	0.012 ± 0.010
M2-54	104−06°1	0.85 ± 0.29	1.00 ± 0.10	4.3	0.10 ± 0.02	0.00 ± 0.00
M4-18	146+07°1	0.69 ± 0.30	0.85 ± 0.10	4.00	0.10 ± 0.02	0.00 ± 0.00
Me 2-2	100−08°1	0.21 ± 0.02	1.02 ± 0.10	3.91	0.148 ± 0.010	0.00 ± 0.00
Na 1	18+20°1	0.09 ± 0.09	1.06 ± 0.1	3.0	0.20 ± 0.10	0.004 ± 0.000
Sn 1	13+32°1	0.22 ± 0.03	0.98 ± 0.05	3.49	0.083 ± 0.010	0.002 ± 0.00
Vy 1-1	118−08°1	0.96 ± 0.4	1.12 ± 0.10	3.3	0.14 ± 0.02	0.00 ± 0.00
Vy 1-2	53+24°1	0.06 ± 0.04	0.93 ± 0.05	3.90	0.078 ± 0.010	0.019 ± 0.000
Vy 2-2	45−02°1	1.48 ± 0.05	1.49 ± 0.20	3.00	0.116 ± 0.030	0.003 ± 0.000
Vy 2-3	107−13°1	0.19 ± 0.10	1.30 ± 0.30	...	0.092 ± 0.020	0.006 ± 0.001

[a] Perek and Kohoutek 1967.

TABLE 2

PHOTOMETRY OF COMPACT PLANETARY NEBULAE

Object (1)	Aperture (2)	log $F(H\beta)$[a] (3)	CS/TC (B) (4)	CS/TC (V) (5)	B (6)	V (7)	Number of Observations (8)	Notes (9)
NGC 650	40″	−11.360	0.354	0.309	$16.10^{+0.48}_{-0.37}$	$15.87^{+0.39}_{-0.30}$	1	1 (40″)
NGC 1360	40″	−10.843	0.998	0.997	10.86 ± 0.01	11.35 ± 0.01	1	1 (4′)
NGC 1501	40″	−11.524	0.740	0.650	15.11 ± 0.12	14.45 ± 0.10	1	
NGC 1514	4′	−11.244	0.992	0.990	9.91 ± 0.01	9.40 ± 0.01	1	1 (16″), 2
NGC 2392	40″	−10.374	0.899	0.846	10.35 ± 0.02	10.53 ± 0.02	2	1 (40″)
NGC 2440	40″	−10.518	...	0.15:	...	$14.3^{+0.9}_{-0.2}$	2	
NGC 6058	40″	−11.802	0.929	0.885	13.55 ± 0.03	13.78 ± 0.07	3	1 (30″) 2
NGC 6210	4′	−10.078	0.506	0.312	12.40 ± 0.14	$12.90^{+0.33}_{-0.31}$	1	2
NGC 6309	40″	−11.162	0.468	0.637	$14.79^{+0.19}_{-0.17}$	$13.74^{+0.17}_{-0.15}$	1	
NGC 6537	40″	−11.633	0.38:	...	>16.1	...	1	2
NGC 6543	40″	−9.564	0.593	0.406	$10.87^{+0.18}_{-0.17}$	$11.31^{+0.26}_{-0.21}$	1	1 (4′)
NGC 6629	40″	−10.837	0.810	0.701	$13.03^{+0.06}_{-0.05}$	$12.77^{+0.07}_{-0.06}$	1	2
NGC 6644	40″	−11.001	...	0.08:	...	>15.9	1	
NGC 6751	40″	−11.258	0.772	0.674	14.10 ± 0.08	13.89 ± 0.09	1	2
NGC 6807	30″	−11.413	0.30:	...	>15.5	...	1	2
NGC 6818	40″	−10.446	0.05:	...	>15.0	...	1	1 (40″)
NGC 6826	4′	−9.966	0.828	0.731	10.22 ± 0.10	10.69 ± 0.10	1	
NGC 6881	30″	−12.251	0.715	0.451	$16.8^{+0.7}_{-0.4}$	$16.7^{+0.6}_{-0.4}$	1	
NGC 6884	30″	−11.110	0.28:	0.10	$16.1^{+1.2}_{-0.7}$	>15.6	1	
NGC 6891	40″	−10.675	0.817	0.716	$12.13^{+0.04}_{-0.05}$	$12.41^{+0.05}_{-0.06}$	1	
NGC 7008	40″	−11.507	0.854	0.827	$13.79^{+0.18}_{-0.16}$	13.21 ± 0.05	1	
NGC 7026	30″	−10.934	0.408	0.459	$15.33^{+0.27}_{-0.25}$	$14.20^{+0.16}_{-0.15}$	1	1 (40″)
NGC 7354	40″	−11.597	...	0.15:	...	>16.2	1	
NGC 7662	40″	−9.956	0.134	0.161	$13.6^{+1.2}_{-0.8}$	$13.2^{+0.5}_{-0.4}$	1	1 (30″)
IC 289	40″	−11.784	0.54:	0.23:	>15.1	>15.9	2	3
IC 418	40″	−9.618	0.760	0.618	10.13 ± 0.05	10.33 ± 0.08	3	
IC 2003	30″	−11.200	0.265	0.132	$16.2^{+0.6}_{-0.5}$	$16.5^{+1.0}_{-0.6}$	2	2
IC 2149	40″	−10.548	0.884	0.798	11.28 ± 0.03	11.59 ± 0.07	1	
IC 2165	40″	−10.910	0.06:	>0.01	>15.8	>16.4	2	
IC 3568	30″	−10.770	0.787	0.775	$12.47^{+0.46}_{-0.32}$	12.31 ± 0.04	1	
IC 4593	40″	−10.548	0.919	0.867	11.02 ± 0.01	11.27 ± 0.01	1	
IC 4732	30″	−11.514	0.15:	0.17:	>16.5	>16.2	2	
IC 4776	30″	−10.699	0.54:	0.10:	$13.7^{+1.6}_{-0.6}$	>14.6	1	
IC 5117	30″	−11.388	0.177	0.136	$17.5^{+0.8}_{-0.6}$	$16.7^{+0.6}_{-0.5}$	1	2
A2	40″	−12.501	0.863	0.843	$16.07^{+0.28}_{-0.22}$	$15.85^{+0.18}_{-0.15}$	1	1 (40″), 2
A15	40″	−12.576	0.842	0.674	$16.07^{+0.28}_{-0.22}$	$16.86^{+0.31}_{-0.24}$	1	
A33	76″	−12.538	0.977	0.958	$14.32^{+0.12}_{-0.11}$	$14.74^{+0.15}_{-0.13}$	1	
A43	40″	−12.931	0.981	0.970	14.70 ± 0.04	14.79 ± 0.06	1	
A46	40″	−12.327	0.948	0.929	$14.62^{+0.15}_{-0.13}$	14.87 ± 0.06	1	
A77	40″	−12.431	0.80:	0.764	>16.0	15.68 ± 0.13	1	1 (40″)
A79	40″	−12.995	0.97:	0.988	>15.4	14.09 ± 0.02	1	
Ha 3-29	40″	−12.508	0.66:	0.1:	>17.0	>18.1	1	
HB 12	30″	−10.966	0.397	0.378	$15.2^{+0.8}_{-0.7}$	$14.3^{+0.6}_{-0.5}$	1	1 (40″)
Hu 1-2	40″	−11.183	...	0.12:	...	$16.1^{+1.3}_{-0.6}$	1	
Hu 2-1	40″	−10.763	0.660	0.513	13.45 ± 0.10	13.63 ± 0.10	1	2
J320	40″	−11.398	0.752	0.653	14.40 ± 0.09	14.44 ± 0.07	2	
J900	30″	−11.225	0.243	0.170	$16.46^{+0.51}_{-0.45}$	$16.26^{+0.81}_{-0.52}$	1	1 (16″)
K3-63	40″	−13.027	0.968	0.961	$15.78^{+0.34}_{-0.26}$	15.12 ± 0.03	1	2
M1-2	40″	−12.050	...	0.951	>12.8	>13.13	1	3
M1-4	40″	−12.208	...	0.519	...	$16.7^{+1.0}_{-0.5}$	1	
M1-11	40″	−11.846	0.886	0.847	15.08 ± 0.08	$14.04^{+0.11}_{-0.10}$	1	
M2-51	40″	−12.238	0.954	0.960	14.76 ± 0.03	13.45 ± 0.02	1	
M2-54	30″	−11.976	0.989	0.983	12.29 ± 0.04	12.10 ± 0.02	1	
M4-18	40″	−11.880	0.956	0.932	14.22 ± 0.05	13.96 ± 0.04	1	2
Me 2-2	16″	−11.174	0.392	0.213	$15.41^{+0.56}_{-0.42}$	$16.08^{+0.52}_{-0.46}$	1	
Na 1	40″	−11.963	0.740	0.48:	$15.8^{+0.7}_{-0.4}$	>16.0	1	
Sn 1	40″	−11.685	0.856	0.768	14.34 ± 0.06	14.70 ± 0.04	1	
Vy 1-1	30″	−11.536	0.858	0.677	14.11 ± 0.09	$14.45^{+0.11}_{-0.10}$	1	
Vy 1-2	16″	−11.527	0.238	0.145	$17.3^{+0.6}_{-0.4}$	$17.6^{+1.3}_{-0.6}$	2	
Vy 2-2	30″	−11.577	0.546	0.536	$15.94^{+0.26}_{-0.22}$	$14.84^{+0.15}_{-0.14}$	1	2
Vy 2-3	30″	−11.955	0.879	0.812	14.56 ± 0.10	14.90 ± 0.10	1	1 (40″)

NOTES.—(1) Confirming, though less precise measurement with the aperture indicated. (2) Possible contamination of flux from field stars. (3) Definite contamination of flux from field stars: magnitude used is an upper limit only.

[a] The values listed here represent only the flux observed within the aperture and are not necessarily total fluxes from the object.

of excitation, nebular size, and He/H = 0.10 (unless He^{2+}/H^+ in known to be higher from the He II λ4686 flux). However, in these cases the uncertainties assigned to each quantity are relatively great and will be reflected in the uncertainties in the magnitudes if the correction for the nebular continuum is also large. Finally, the λ5500 filter passes some weak nebular lines, notably He II λ5411 and [Cl III] λλ5417, 5437, which were removed in the reduction.

We present the derived magnitudes in Table 2. Columns (1) and (2) list the object and the aperture used for the photometry, and column (3) contains the log of the observed Hβ flux within that aperture (we emphasize here that these are *not* necessarily total Hβ fluxes). Columns (4) and (5) give the (calculated) contribution of the central star (CS) as a fraction of the total observed continuum (TC) at *B* and *V*, respectively, while columns (6) and (7) contain the resulting stellar *B*- and *V*-magnitudes with the associated errors. Column (8) gives the number of observations of each object, followed by notations of any special circumstances in column (9). Note especially comments b and d, which indicate the degree of contamination of the data from field stars.

We took special care with the calculation of realistic uncertainties in the stellar magnitudes. The uncertainty associated with each nebular parameter was propagated through the equation for the effective continuum recombination coefficient as given by Brown and Mathews (1970). We then combined quadratically the resulting uncertainty in the nebular continuum with those in the Hβ and continuum fluxes (from photon statistics) to give the total uncertainty associated with the derived stellar flux. The only exceptions to this procedure occurred in cases for which the electron density was greater than 10^4 cm^{-3}. At this threshold we arbitrarily increased the uncertainty in *x*, the probability per recombination for 2 quantum emission, to allow for collisional repopulation of the metastable atomic levels. If N_e is not given in Table 1, it is assumed to be low. Finally, the errors associated with the standard star magnitudes are negligible, and are ignored.

III. COMPARISON OF MAGNITUDES

In this section we compare our data with a variety of other magnitude determinations in order to test them for systematic error. We consider three sets of data: (1) the extensive list circulated by Shao and Liller (1973, hereafter SL), now cataloged by Acker *et al.* (1982); (2) other photoelectric measurements, principally those by Kostjakova *et al.* (1968); and (3) the numerous photographic determinations found in Perek and Kohoutek (1967). Since the SL list is the one most comparable to ours, we consider it first.

a) Comparison with Data of Shao and Liller

Schönberner (1981) noted the systematic difference between the central-star magnitudes published by Kaler (1976*a*, 1978) and SL. In Figure 1 we illustrate this discrepancy by plotting the magnitudes listed in Table 2 against theirs. The data in this figure show that our values are systematically fainter than SL's by about 1 mag at essentially all flux levels, and we consider this discrepancy to be due almost entirely to an inadequate accounting, on the part of SL, for the nebular contribution to the continuum. Figure 2 shows the difference in magnitudes between the results of the present work and those of SL plotted as a function of the fractional stellar contribution to our total (nebular plus stellar) measured continuum flux, also expressed in magnitudes. The solid line indicates the correlation that

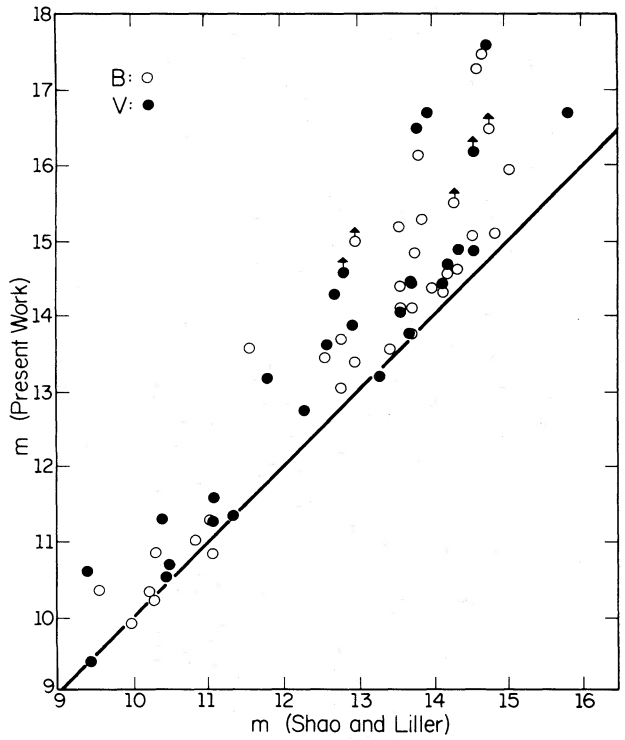

FIG. 1.—Measured stellar magnitudes from the present work plotted against the stellar magnitudes from SL for central stars in common. Solid line is the 1:1 slope.

would be expected if the SL magnitudes were contaminated by the nebular continuum flux. The plotted points follow the expected relation qualitatively well. If anything, we might expect the points to fall below the line because of the smaller apertures used by SL (which should result in lower contamination). That the points fall systematically about ¼ mag *above* the line indicates a small additional source of error that may affect either of the studies. It is nonetheless clear that the discrepancy between the present work and the SL magnitudes results largely from the nebular contribution to the total continuum.

It should be emphasized, however, that the SL magnitudes are quite accurate for the cases in which the nebular contribution to the continuum is small. Unfortunately, the degree of the continuum contribution cannot be evaluated easily without a detailed analysis such as the one presented above, which requires a rather extensive knowledge of the nebular parameters. Ideally, one would like to apply a correction to the published magnitudes in order to make best use of the available data. In principle, one could use published total Hβ fluxes and adopt reasonable nebular parameters to derive the nebular contribution to SL's total magnitudes. However, the results will be inaccurate unless the nebula is angularly significantly smaller than the aperture used for the continuum measurements, which, in the case of SL, was often only a few arcseconds (Liller 1984).

As a safe alternative to the above scheme, and in lieu of additional photometry, one could entirely avoid using SL continuum magnitudes that have a high probability of suffering nebular contamination. Unfortunately, no single nebular parameter scales precisely with the nebular continuum, for the continuum is a complicated function of nebular morphology

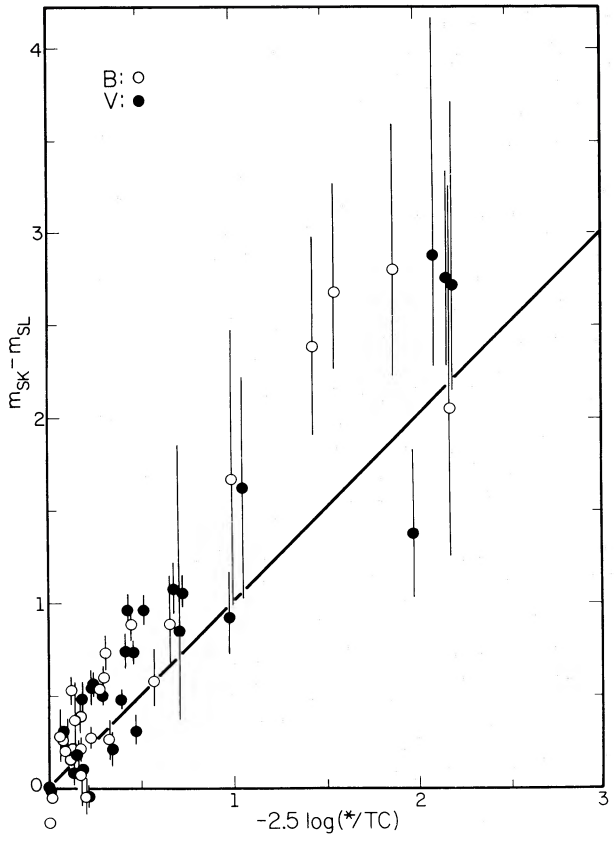

FIG. 2.—Difference between the stellar magnitudes from the present work and those from SL plotted against the fractional stellar contribution to the total (nebular + stellar) measured flux expressed in magnitudes. Solid line shows the correlation to be expected if the SL magnitudes were contaminated by the nebular continuum flux.

and evolution, electron temperature, Hβ surface brightness, and so on, and this complexity compounds the problem of deciding what criteria to use to discern the accuracy of the SL magnitudes. Nonetheless there are some general trends. For example, Figure 3 shows the difference between our magnitudes and those of the SL sample plotted against the log of the nebular angular radius (taken mostly from Perek and Kohoutek 1967). These data suggest a correlation in the sense of an upper envelope boundary: the SL magnitudes for the central stars of those nebulae with $\phi > 40''$ probably do not suffer from significant nebular contamination, while those with $\phi < 10''$ almost certainly do, and those in the intermediate range ($10'' \leq \phi \leq 40''$) *may* be markedly too bright. Unfortunately, most planetary nebulae, and indeed most of the SL sample, are angularly small, so that the above relation is not very selective.

Another such relation exists for the physical nebular radii, although it is less well-defined. The suggestion here is that SL's magnitudes for the central stars of nebulae with radii greater than about 0.16 pc suffer little from contamination, which is roughly consistent with Kaler's (1983*b*) definition of large (i.e., well-evolved) planetary nebulae. Finally, we find that nebulae with dereddened log Hβ surface brightnesses greater than $\sim 10^{-14}$ ergs cm^{-2} s^{-1} arcsec^{-2} may also contribute heavily to the continuum flux.

b) Other Photoelectric Determinations

We now compare our data with other photoelectric determinations, in order to substantiate our conclusions of the previous subsection. Outside of SL, our greatest overlap is with Kostjakova *et al.* (1968), who measured *UBV* magnitudes of the central stars of 24 nebulae. These, along with some from Abell (1966), two from Méndez, Kudritzki, and Simon (1984), and a limit from Reay *et al.* (1984), are plotted against our magnitudes in Figure 4. We also replot SL magnitudes against ours for the nuclei of three nebulae with $\phi > 40''$ which, according to the last subsection, should be uncontaminated by nebular continuum.

Up to about magnitude 14.3, the 45° slope acts as a lower envelope to the plotted points, that is, our magnitudes are greater than or equal to (allowing for some random error) the others. This effect is just what we would expect if the other measurements are afflicted with line and/or continuum contamination. Kostjakova *et al.* (1968) in fact point out that two of the nebulae with high surface brightness (NGC 6543 and IC 3568) that are raised above the 45° slope could not be corrected properly for nebular radiation with their technique, and the worst case, NGC 6210, was not corrected at all. One other, IC 418, also has a high surface brightness, and their color for NGC 7008 is far too negative for its high extinction (see Kaler and Feibelman 1985), so that the disagreement for *B* can be discounted. That leaves only NGC 6751, for which no explanation is readily at hand. Note also that the SL magnitudes adopted here agree quite well with ours.

At magnitude 14.3, the points begin to scatter below the line, suggesting that our measures of stellar flux are too large. We consider the Abell (1966) magnitudes to be excellent; the two points by Méndez, Kudritzki, and Simon (1984) should be

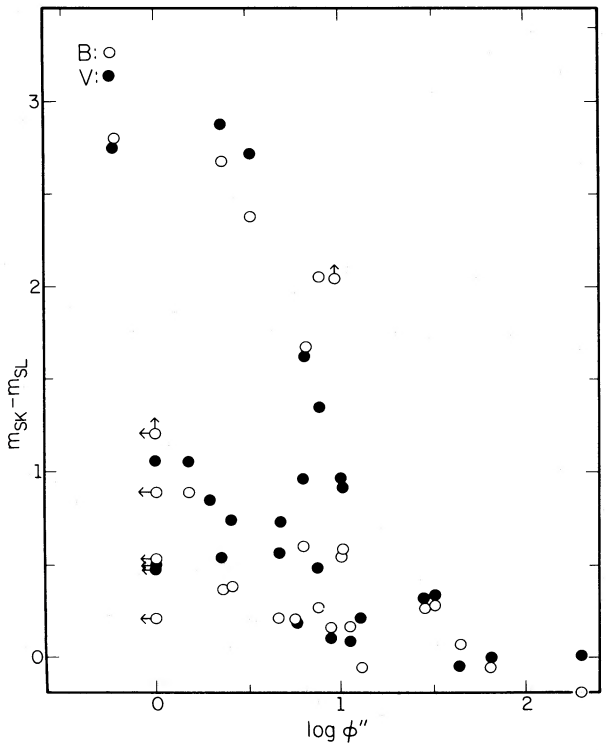

FIG. 3.—Difference between our stellar magnitudes and those of SL plotted against the log of the nebular angular radius in arcseconds.

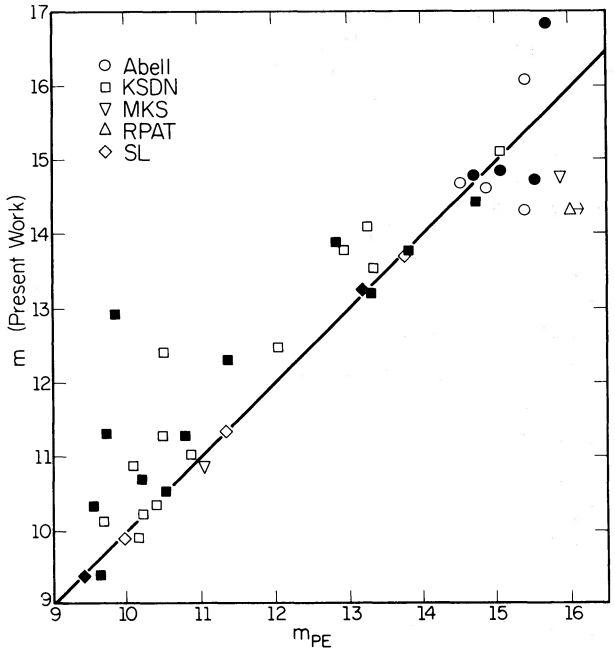

FIG. 4.—Various other photoelectric magnitudes plotted against ours. *Circles:* Abell (1966); *boxes:* Kostjakova *et al.* (1978); *inverted triangles:* Méndez, Kudritzki, and Simon (1984); *triangle:* Reay *et al.* (1984); *diamonds:* Shao and Liller (1973) for nebulae with $\phi \geq 40''$; *open symbols:* *B*-magnitudes; *filled symbols:* *V*-magnitudes. Solid line is the 1:1 slope.

accurate as well, as is the limit on NGC 2440 from Reay *et al.* (1984). It is our data that now appear unreliable. Another case in point in NGC 6537, not plotted, for which we and Reay *et al.* (1984) give $B = 16.7$ and $V = 19.0$, respectively (our large error bar, however, nearly encompasses their value). Note also that most of our lower limits occur in the neighborhood of $m \approx 15$. *The reader should thus be aware that our stated magnitudes over* ~ 14.3 *may also be lower limits.*

An additional check on the reliability of our technique stems from a comparison of our data for NGC 7662 with a nebular model constructed by Harrington *et al.* (1982) based upon observations made with the *International Ultraviolet Explorer* (*IUE*). Although the stellar continuum fluxes they predict are somewhat smaller than ours (by ~ 0.2 mag at *B* and ~ 0.8 mag at *V*), they adopt different nebular parameters from those in Table 1. In particular, their modeled electron temperature distribution differs in the mean from our value. In this case, the most important comparison is the fraction of stellar to total continuum, for which they find 16% at *B* and 9% at *V* as against our 13% at *B* and 16% at *V*. Although our large error bars just permit agreement, theirs are clearly the better values. It is also clear that our magnitudes are least reliable when the stellar contribution to the continuum is less than about 15% of the total. Nonetheless, our magnitudes for this object are clearly superior to others in the literature to date, in spite of the errors. We note again here that these data were acquired primarily for wide-aperture study of the nebulae, not for examination of the nuclei. Further work will employ smaller apertures in order to extend this survey more deeply.

c) Colors

We now compare our magnitudes with one another in the form of $B-V$ colors, and compare these with the nebular extinctions of Table 1 in order to gain further insight into the accuracy of the data. The two quantities are plotted against one another in Figure 5, where, in view of the comments of the preceding subsection, we isolate the stars for which either *B* or *V* is greater than 14.3 (indicated by filled symbols). The solid line is the relation expected for a reddened, hot blackbody with $(B-V)_0 = -0.38$, and the Whitford (1958) reddening function, which leads to $c = 1.41E(B-V)$ (see Kaler and Feibelman 1985).

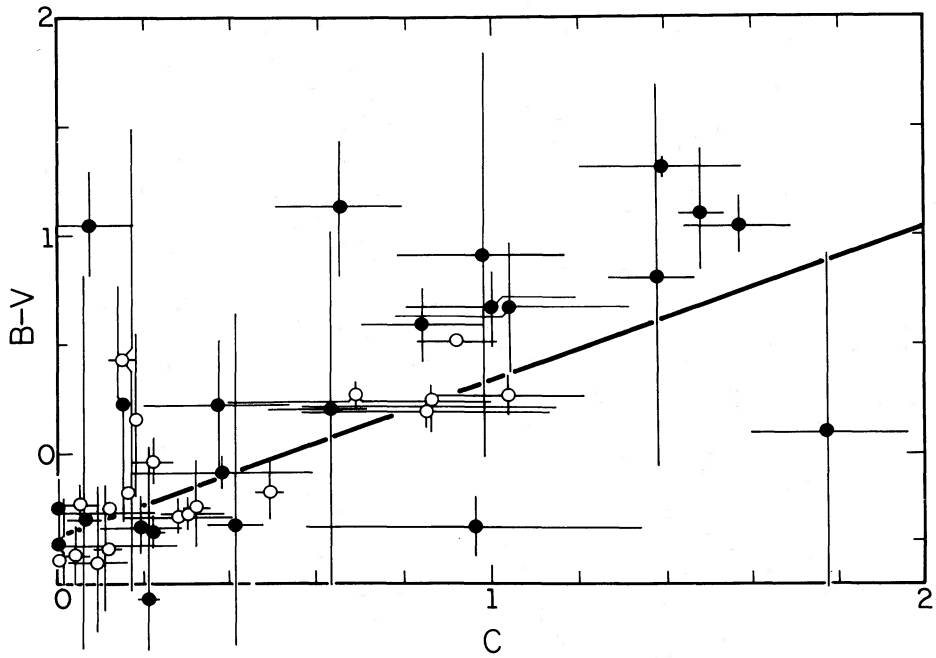

FIG. 5.—$B-V$ colors computed from Table 2, plotted against nebular extinction *c* from Table 1. *Open circles: B and V* both <14.3; *filled circles: B or V* >14.3; *line:* expected correlation for $(B-V)_0 = -0.38$ and $c = 1.41E(B-V)$.

We see that for the most part the points follow the trend of the line, and are consistent with it to within the error bars. However, some of the data vary widely from the expected relation by nearly a full magnitude in $B-V$ color. These data belong almost exclusively to the fainter set described in the last subsection. However, many of these *are* consistent with the line, and we simply caution the reader that our data for this fainter set *may* be erroneous.

d) Photographic Magnitudes

The most extensive magnitude measurements are still those derived from the older photographic data. We therefore compared several sets of these with ours: the results for determinations by Hubble, van Maanen, Anderson, and Kohoutek (see Perek and Kohoutek 1967 or Acker *et al.* 1982) are plotted in Figure 6. We see that the 45° line does not pass through the point distribution, but rather defines a sharp upper limit, with the photographic values being, on the average, $\frac{3}{4}$ mag too bright. In view of the earlier discussion, the origin of the offset certainly lies with the older data. Some of it is likely caused by the calibration difference between photographic blue magnitudes and B, and some by the difficulty of estimating the brightness of an image against a luminous nebular background. In addition, strong nebular radiation probably tends to hypersensitize a photographic plate, which can make stars appear somewhat brighter than they really are.

We confirm the discrepancy by plotting in Figure 7 Kohoutek's photographic blue magnitudes (from Perek and Kohoutek 1967) against both the photographic and photoelectric values of Abell (1966). Again, we see that the photographic values are measured as too bright compared with the photoelectric values, especially for magnitudes brighter than $m = 16$, the range considered in this paper. The offsets in Figures 6 and 7 agree quite well. However, the two photographic sets show good agreement, so that the systematic shift may affect the photographic Abell values as well. We conclude that these photographic data sets are acceptable for use after adding on the average 0.75 mag, with a resulting precision of roughly ± 0.75 mag.

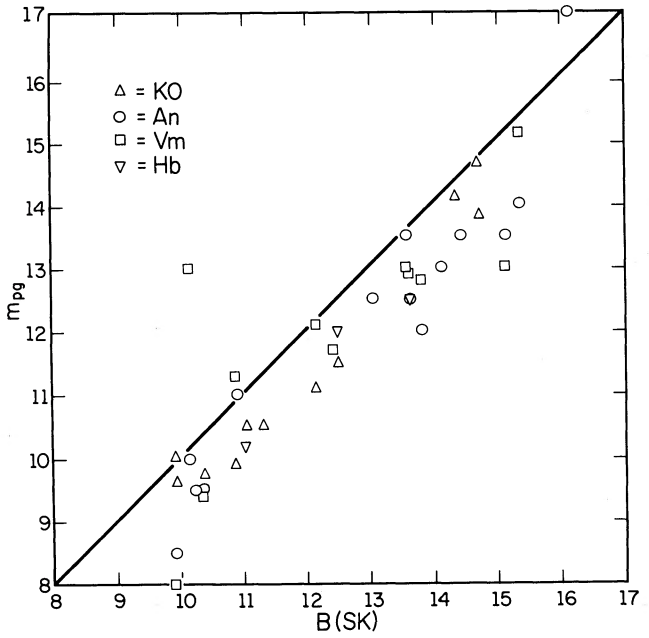

FIG. 6.—Photographic blue magnitudes plotted against B from Table 2. Measurements, taken from Perek and Kohoutek (1967) or from Acker *et al.* (1982), made by Anderson (*circles*), Kohoutek (*triangles*), van Maanen (*boxes*), and Hubble (*inverted triangles*). The line is the 1:1 slope.

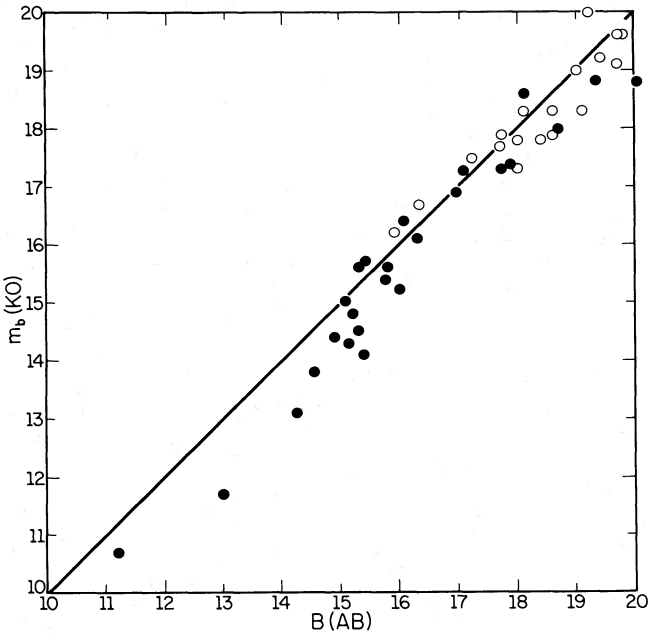

FIG. 7.—Photographic blue magnitudes for Abell nebulae by Kohoutek, from Perek and Kohoutek (1967), plotted against Abell's (1966) photographic blue (*open circles*) or photoelectric B (*filled circles*) magnitudes. This figure is to be compared with Fig. 6 to show the similar downward offset of points in the magnitude range covered by this paper.

IV. ANALYSIS

We use our new data to calculate Zanstra temperatures and luminosities in order to begin to examine the distribution of our set of stars on the log L–log T plane. The analysis uses the nebular data (extinction, and absolute Hβ and He II λ4686 fluxes) from this work and from those cited in § II and in Cahn and Kaler (1971), whose distance scale, modified for improved data, is used as well. Although it is clear that we should adopt separate distance scales for nebulae in different states of optical thickness (Maciel and Pottasch 1980; Daub 1982), the observational distinction between them is currently ambiguous. The distance scales described above need further scrutiny, and we do not wish, on the basis of our present sample, to comment on the propriety of the various approaches. Such an analysis will be included in a later paper, wherein we will combine our work with other reliable data for a full examination of evolution. Note that if the nebulae are thick, which most of the low-excitation objects likely are, the distances and luminosities are *upper limits*. The subsequent analysis closely parallels that of Kaler (1983*b*), who provides additional details.

The results for most of the nuclei are presented in Table 3. The first two columns contain the object name and the angular diameter in arc seconds, respectively, while columns (3) and (4) give the calculated distance in kpc and the nebular radius in pc (based upon ϕ and D), respectively. Column (5) gives the calculated Zanstra temperature, based upon He II unless otherwise noted, and column (6) gives the ratio of the He II to the hydrogen Zanstra temperature (TR), where applicable, which is a measure of the optical depth of the nebula to Lyman radiation.

TABLE 3

TEMPERATURES AND LUMINOSITIES

Nebula (1)	ϕ (arcsec) (2)	D (kpc) (3)	R (pc) (4)	T (K) (5)	TR (6)	$L/L_\odot$ (7)
NGC 650	36	1.10	0.19	133^{+13}_{-11}	$1.41^{+0.30}_{-0.25}$	367^{+71}_{-82}
NGC 1360[a]	198	0.35	0.33	>82	2.49 ± 0.15	>540
NGC 1501	29	1.02	0.14	96 ± 3	2.24 ± 0.14	3800 ± 640
NGC 1514	64	0.64	0.20	51 ± 3	2.60 ± 0.14	15600 ± 3300
NGC 2392	9	2.43	0.11	65 ± 1	2.54 ± 0.06	36400 ± 1500
NGC 2440	8.1	2.27	0.09	112^{+16}_{-4}	$1.85^{+0.58}_{-0.14}$	7540^{+2360}_{-4050}
NGC 6058	11.2	3.69	0.20	70 ± 1	2.66 ± 0.06	5480 ± 1430
NGC 6210	8.4	2.10	0.08	67 ± 2	$1.29^{+0.11}_{-0.09}$	3250^{+600}_{-680}
NGC 6309	8.9	3.44	0.15	87 ± 8	2.21 ± 0.41	4200^{+1750}_{-1760}
NGC 6537[b]	5.1	2.14	0.05	>93	...	<69200
NGC 6543[c]	10.3	1.46	0.07	48 ± 3	...	<2950
NGC 6629[c]	7.5	2.08	0.08	35 ± 1	...	<4880
NGC 6644[b]	1.3	8.40	0.05	>68	...	<16800
NGC 6751	10	2.27	0.11	76 ± 3	2.14 ± 0.10	9240 ± 4190
NGC 6818[b]	9.4	2.11	0.10	>111	...	<4120
NGC 6826[c]	12.8	1.54	0.10	35 ± 1	...	<2140
NGC 6881	1.6	7.15	0.06	77^{+7}_{-5}	$2.04^{+0.37}_{-0.27}$	61200^{+26100}_{-33200}
NGC 6884[d]	2.6	4.87	0.06	<112	...	11000 ± 7900
NGC 6891[c]	7.6	2.61	0.10	34 ± 1	...	<2230
NGC 7008	44	0.78	0.17	96 ± 3	$2.40^{+0.16}_{-0.15}$	3200 ± 750
NGC 7026	11	2.00	0.11	80 ± 5	1.47 ± 0.26	2610 ± 1030
NGC 7354[b]	10	1.75	0.08	>96	...	<9290
NGC 7662	7.8	2.04	0.08	113^{+17}_{-13}	$1.60^{+0.58}_{-0.42}$	7810^{+2410}_{-3260}
IC 289[b]	18	1.74	0.15	>85	...	<7600
IC 418[c]	6.3	1.77	0.05	42 ± 2	...	$<8050 \pm 490$
IC 2003	3.3	5.29	0.08	111^{+15}_{-10}	$1.63^{+0.49}_{-0.32}$	6020^{+1670}_{-2460}
IC 2149[c]	4.7	3.38	0.08	31 ± 1	...	<5860
IC 2165[b]	4.0	4.01	0.08	>112	...	<6610
IC 3568	3.5	4.75	0.08	52 ± 1	$1.61^{+0.12}_{-0.10}$	13210^{+2590}_{-2930}
IC 4593[c]	5.7	3.30	0.09	28 ± 0	...	<3860
IC 4732[b,c]	1.5	9.57	0.07	>50	...	<3880
IC 4776[c]	4.0	3.64	0.07	46 ± 20	...	<6280
IC 5117	0.6	0.78	0.03	92^{+9}_{-7}	$1.22^{+0.33}_{-0.26}$	68000^{+24000}_{-29300}
A2	15	3.74	0.27	75 ± 4	$2.46^{+0.19}_{-0.18}$	1260^{+390}_{-410}
A15[a]	17.0	4.23	0.35	>80	...	>420
A33	134	0.73	0.47	84 ± 9	2.17 ± 0.44	107 ± 55
A43[d]	40	2.10	0.41	<70	2.80 ± 0.01	<1280
A46[d]	32	2.22	0.34	<59	...	<400
A77[a]	21	1.25	0.13	>59	...	>4570
A79[c]	27	1.82	0.24	22 ± 2	...	<1680
Ha 3-29[b]	7	4.32	0.15	>87	...	<9310
Hu 1-2	2.5	5.57	0.07	122^{+28}_{-13}	$1.91^{+0.93}_{-0.41}$	18700^{+6000}_{-12200}
Hu 2-1	1.5	6.81	0.05	52 ± 2	1.26 ± 0.07	19000 ± 2900
J320	4.8	5.03	0.12	60 ± 3	1.63 ± 0.10	3510 ± 650
J900	4.5	4.25	0.09	102^{+10}_{-8}	$1.67^{+0.38}_{-0.28}$	4970^{+1570}_{-1990}
M1-4	2.0	7.15	0.07	>69	$1.82^{+0.52}_{-0.29}$	<27900
M4-18[c]	2	13.08	0.06	27 ± 1	...	<15900
Me 2-2[c]	0.6	6.08	0.05	58^{+11}_{-8}	...	<10800
Sn 1	[e]	<4.95	>0.07	54 ± 2	1.73 ± 0.08	<26500
Vy 1-1	2.6	8.43	0.11	56 ± 5	1.70	6440 ± 1760
Vy 1-2	2.3	8.95	0.10	104^{+15}_{-8}	$1.38^{+0.50}_{-0.26}$	2280^{+610}_{-1200}
Vy 2-2	[e]	<7.77	>0.04	63 ± 6	1.52 ± 0.18	<96700
Vy 2-3	2.3	10.37	0.12	60 ± 2	2.06 ± 0.08	10900 ± 1900

[a] He II λ4686 flux is greater than 0.90 times that from Hβ, indicating that the temperature and luminosity are both lower limits.

[b] L and T based upon a limiting magnitude, so that L is an upper limit and T is a lower limit.

[c] Object has no detectable He II flux: calculations for L and T are based on hydrogen. L is expected to be an upper limit.

[d] Temperature and luminosity are based on an upper limit to the He II flux and are therefore also upper limits.

[e] Angularly unresolved planetary. The luminosity is therefore an upper limit.

If TR $\lesssim$ 1.2, we consider the nebula to be optically thick in the hydrogen Lyman continuum; if it is very high, $\gtrsim$2.5 (and He II λ4686 is stronger than $\sim$0.9 times Hβ), it is likely to be optically thin in the He^+ Lyman continuum, and T_z(He II) is a lower limit. Finally, column (7) gives the stellar luminosity based on the calculated distance, temperature, and stellar magnitudes. Note again that we consider L to be an upper limit if He II is not present in the nebular spectrum, or if TR $\lesssim$ 1.2.

The central stars and their evolutionary tracks for various masses are plotted on the log L–log T plane shown in Figure 8. The 0.546, 0.565, 0.598, and 0.644 $M_\odot$ tracks are from Schönberner (1983), the 0.80 and 1.20 $M_\odot$ tracks are from Paczyński (1971), and the estimate for 1.4 $M_\odot$ is from Shaw, Truran, and Kaler (1984). Each central star is coded according to its contribution to the total (nebular plus stellar) observed continuum at B and V. Limiting values for L and T as discussed above are indicated by arrows. Finally, an arrow originating from Vy 2-3 near the center of the plot indicates the displacement necessary were the stellar continuum 1 mag fainter, illustrating the systematic shift in L and T that would occur if a corresponding amount of nebular contamination were present. The direction of the shift depends somewhat upon the stellar temperature, but it is not qualitatively different than that shown.

Although the sample of planetary nuclei presented here is certainly not in any sense complete, we can draw general conclusions about the studies that have been made to date about their evolution. In particular, it is clear from Figure 8 (as it is from earlier discussion) that the planetary nebula nuclei (PNNs) that are hottest and/or most luminous also tend to be those that suffer the greatest continuum contamination from the surrounding nebula. Furthermore, no PNN in this sample has an effective surface temperature that is unambiguously hotter than about 130,000 K. These related findings are, of course, consistent with evolutionary scenarios for young planetaries surrounding nuclei that rapidly evolve to high surface temperature at constant high luminosity: the nucleus fades at optical wavelengths as its radiation becomes harder, while the nebula brightens in response to the increasing Lyman radiation and (if it is ionization-bounded) to the increasing amount of ionized matter in the shell. Unfortunately, these effects combine to confound the analysis of the observational data by reducing the contrast between the nebular and stellar flux. The

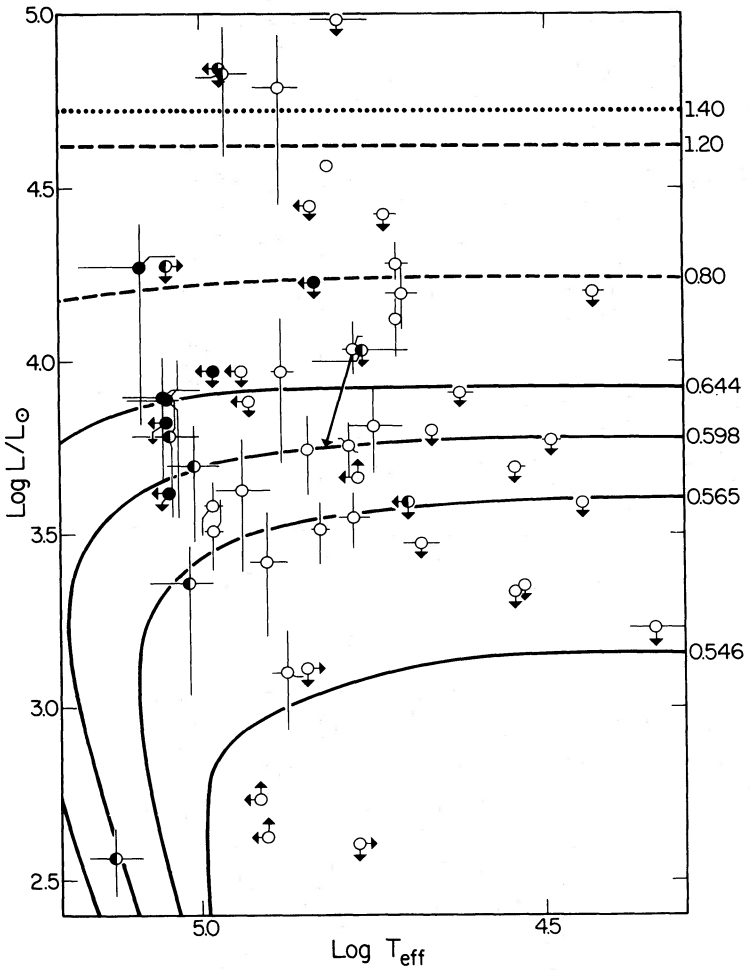

FIG. 8.—Distribution of the planetary nebula nuclei on the log L–log T plane from Table 3. Solid curves are the Schönberner (1983) evolution tracks for 0.546, 0.565, 0.598, and 0.644 $M_\odot$ cores; dashed curves are the Paczyński (1971) tracks for 0.8 and 1.2 $M_\odot$ cores; dotted curve is the limiting 1.4 $M_\odot$ core estimated by Shaw, Truran, and Kaler (1984). Filled circles indicate those objects whose total (nebular and stellar) flux exceeded the CS by $\geq$2.0 mag; half-filled circles indicate those objects whose total flux exceeded the CS by 1.0–2.0 mag. The arrow originating from Vy 2-3 indicates the displacement if the stellar continuum were 1 mag fainter, illustrating the effect of adopting uncontaminated magnitudes.

apparent lack of the hottest PNN (those with surface temperatures greatly exceeding 130,000 K) is almost certainly due in part to the difficulty heretofore of distinguishing between the stellar and nebular continua. It would appear, then, that a great deal more spectrophotometry of young, compact planetary nebulae and their nuclei is in order—not simply to increase the accuracy of the calculated stellar parameters, but also to provide a crucial tool for studying the hottest phases of PNN evolution.

V. SUMMARY

The data presented in this paper were not, in general, obtained with the intention of determining the continuum flux at B and V of the central stars of planetary nebulae (which resulted, in some cases, in rather large formal errors on the magnitudes). However, the magnitudes presented here are usually the best available for these objects, if only because the often large correction to the magnitudes for the contribution from the nebular continuum has been underestimated or ignored by many investigators. In addition to outlining the procedure for calculating the correct stellar continuum, we have presented all of the nebular parameters that we adopted in the calculation, so that any subsequent improvement in the knowledge of any one of them can also allow an improvement of the central-star magnitudes. Herein lies the major disadvantage of this method: a large amount of information must be derived from rather extensive data in order to calculate accurately the nebular contribution to the continuum. Nonetheless, the correction must be made—if only approximately—from best estimates of the physical parameters of the nebulae if we are to study planetary nuclei and their evolution. It should be emphasized that the continuum problem cannot be solved by using imaging techniques alone, as Reay *et al.* (1984) have suggested. Although these methods can be very effective for larger objects, most nebulae are angularly small ($\phi < 5''$), so that continuum contamination becomes an important problem. And the simple photometric technique described herein is the only method available for unresolved planetaries.

Probably the best method for accurately determining the PNN luminosity and temperature is to model the composite (stellar plus nebular) radiation and compare it with ultraviolet and optical observations, as done by Harrington *et al.* (1982). In this way one examines the star at wavelengths that provide better contrast with the nebula, and avoids uncertainties such as the one brought about by the adoption of a mean electron temperature when in fact there is a temperature gradient. Unfortunately, this method requires even more nebular and stellar data than does the relatively simple technique presented here.

Comparison of our results with other photoelectrically derived magnitudes establishes the validity of ours up to about magnitude 14.3. Fainter than this limit, we may underestimate. We have compared our results in detail with magnitudes determined by Shao and Liller (1973) and found that the large systematic difference between our results and theirs is due almost entirely to their lack of correction for the nebular continuum. Closer examination reveals that most SL magnitudes suffer from some degree of nebular contamination (in some cases more than 2 mag)—in particular, for those nebulae with angular radii less than 10″, physical radii less than 0.16 pc, or unreddened log Hβ surface brightnesses greater than 10^{-14} ergs cm^{-2} s^{-1} arcsec^{-2}. Care must be taken in applying a correction to SL magnitudes for nebular continuum, for most of their observations were made with angularly small apertures. Thus, scaling the nebular continuum/Hβ ratio by a total Hβ flux from the literature would not be appropriate for nebulae whose angular diameters approached or exceeded the aperture size used by SL. We also establish the validity of older photographic measurements, and find that they are improved if on the average they are made fainter by 0.75 mag and that their resulting precision is about ± 0.75 mag. Finally, we place the problem of correcting for the nebular continuum in the context of the evolution of planetary nebula nuclei. We conclude that the study of the hottest and brightest nuclei is critically dependent upon that correction, and confirm that the current apparent lack of extremely hot PNNs is due, in part, to a heretofore inadequate accounting for the nebular continuum.

This research was supported by NSF grant AST 80-23233 to the University of Illinois. We would like to thank W. Liller for helpful discussion.

REFERENCES

Abell, G. O. 1966, *Ap. J.*, **144**, 259.
Acker, A., Gleizes, F., Chopinet, M., Marcout, J., Ochsenbein, F., and Roques, J. M. 1982, *Catalogue of the Central Stars of True and Possible Planetary Nebulae* (Pub. Spec. C.D.S., No. 3).
Aller, L. H., and Czyzak, S. J. 1979, *Ap. Space Sci.*, **63**, 397.
Barker, T. 1978, *Ap. J.*, **219**, 914.
Brocklehurst, M. 1971, *M.N.R.A.S.*, **153**, 471.
Brown, A., and Mathews, W. 1970, *Ap. J.*, **160**, 939.
Cahn, J. C., and Kaler, J. B. 1971, *Ap. J. Suppl.*, **22**, 319.
Daub, C. 1982, *Ap. J.*, **260**, 612.
Harrington, J. P., Seaton, M. J., Adams, S., and Lutz, J. 1982, *M.N.R.A.S.*, **199**, 517.
Kaler, J. B. 1976*a*, *Ap. J.*, **210**, 113.
———. 1976*b*, *Ap. J. Suppl.*, **31**, 517.
———. 1978, *Ap. J.*, **226**, 947.
———. 1979, *Ap. J.*, **228**, 163.
———. 1980, *Ap. J.*, **239**, 78.
———. 1983*a*, *Ap. J.*, **264**, 594.
———. 1983*b*, *Ap. J.*, **271**, 188.
———. 1983*c*, *IAU Symposium 103, Planetary Nebulae*, ed. D. R. Flower (Dordrecht: Reidel), p. 245.
———. 1985, *Ap. J.*, **290**, 531.
Kaler, J. B., and Feibelman, W. A. 1985, *Ap. J.*, in press.
Kostjakova, E. B., Savel'eva, M. V., Dokuchaeva, O. D., and Noskova, R. I. 1968, *IAU Symposium 38, Planetary Nebulae*, ed. D. E. Osterbrock and C. R. O'Dell (Dordrecht: Reidel), p. 317.
Liller, W. 1984, private communication.
Maciel, W. J., and Pottasch, S. R. 1980, *Astr. Ap.*, **88**, 1.
Martin, W. 1981, *Astr. Ap.*, **98**, 328.
Méndez, R. H., Kudritzki, R. P., and Simon, K. P. 1984, *Astr. Ap.*, in press.
Paczyński, B. 1971, *Acta. Astra.*, **21**, 417.
Perek, L., and Kohoutek, L. 1967, *Catalogue of Galactic Planetary Nebulae*, (Prague: Czechoslovakia Academy of Sciences).
Reay, N. K., Pottasch, S. R., Atherton, P. D., and Taylor, K. 1984, *Astr. Ap.*, **137**, 113.
Schönberner, D. 1981, *Astr. Ap.*, **103**, 119.
———. 1983, private communication.
Shao, C. Y. and Liller, W. 1973, private communication (SL).
Shaw, R. A., and Kaler, J. B. 1982, *Ap. J.*, **261**, 510.
Shaw, R. A., Truran, J. W., and Kaler, J. B. 1984, *Bull. AAS*, **16**, 530.
Torres-Peimbert, S., and Peimbert, M. 1977, *Rev. Mexicana Astr. Ap.*, **2**, 181.
Webster, B. L. 1969, *M.N.R.A.S.*, **143**, 113.
Whitford, A. E. 1958, *A.J.*, **63**, 201.

James B. Kaler and Richard A. Shaw: Astronomy Department, University of Illinois, 341 Astronomy Building, 1011 W. Springfield Avenue, Urbana, IL 61801-3000